The dorsal medial frontal cortex mediates automatic motor inhibition in uncertain contexts: evidence from combined fMRI & EEG studies - Supplementary Material

Albares M, Lio G, Criaud M, Anton JL, Desmurget M, Boulinguez P

Contents:

---

1. Supplementary figures

Figure S1: Detection of early electrophysiological indices of response inhibition. In order to track the earliest activity evoked by reactive inhibitory processes, a multiple hypothesis testing procedure was designed. For each one of the 134 independent components (IC), the mean evoked activity was estimated both for the go and the go_control conditions in height time-periods of 25ms, from 50ms to 250ms after stimulus onset. A Wilcoxon test ($p<0.05$, Bonferroni corrected) was used to test differences between go and the go_control conditions for each IC and each time period (boxes are filled out when significant). This blind test reports only one component showing early significant differences between the conditions with and without uncertainty (the dMF170 within the SMC). Later, non-overlapping effects are generated within the cuneus, the precuneus and the anterior cingulate cortex (ACC), whose activities more likely account for the classical ERPs N2 and P3 (see Fig. S2).

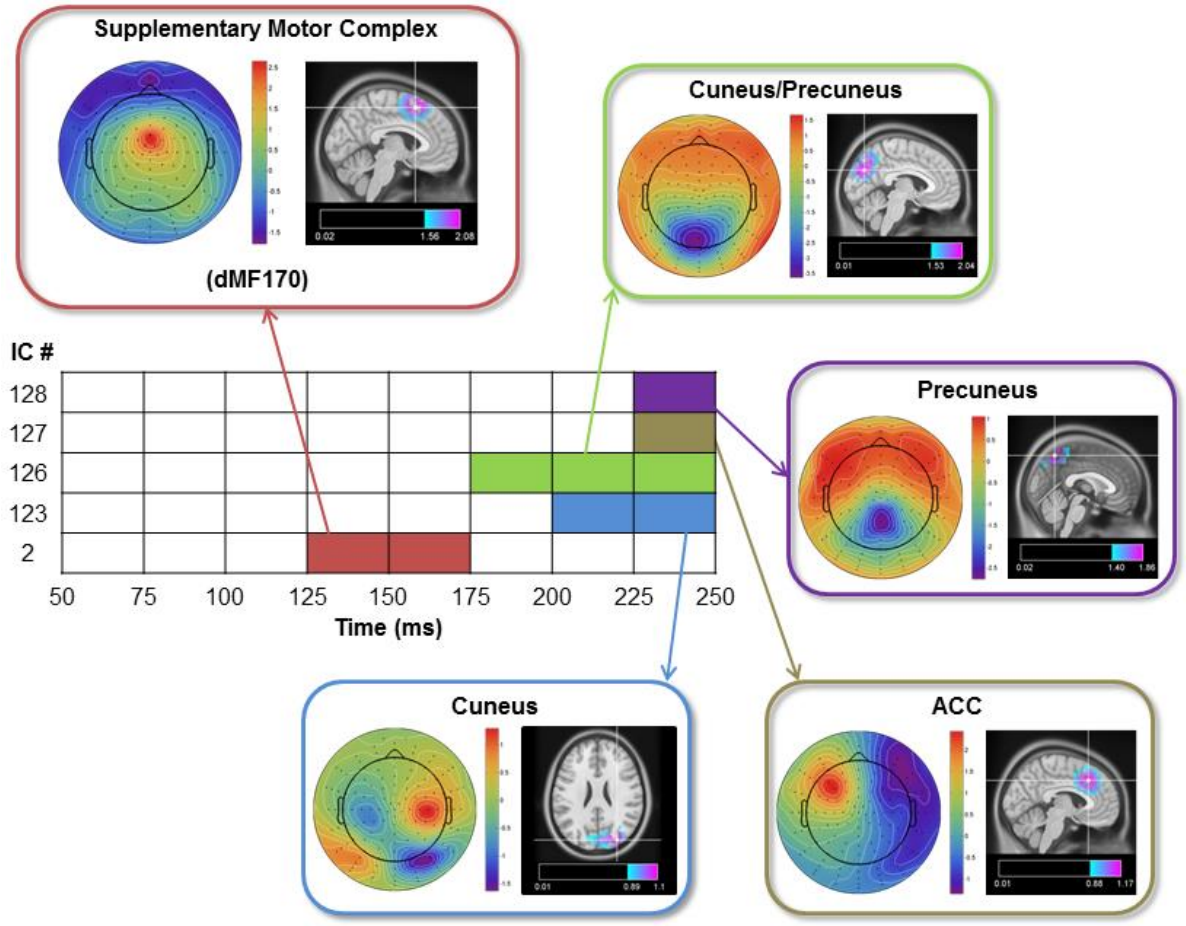

Figure S2: Sources contributing to the N2 and P3, as assessed with the standard [Nogo – Go] contrast. Two main conclusions emerge from this analysis. First, it strongly supports the view that the N2 and the P3 are not unambiguous markers of response inhibition (Huster et al., 2013). The N2 and the P3 are complex ERPs composed of mixed sources of activity originating from synchronized activity of multiple regions ranging from anterior (iFG) to posterior (occipital) parts of the brain (see also Zhang et al., 2014 for similar data). Second, the N2 and the P3 peak relatively late in the timeline of the sensorimotor processes (300 and 440 ms after stimulus onset, respectively, which is 130 and 270 ms after the dMF170). In other words, consistent with the above mentioned studies, it seems unlikely that these ERPs pinpoint actual inhibitory mechanisms because they fall outside the temporal window inside which fast automatic motor responses are triggered (i.e., before which response inhibition must occur). The N2 could rather index the detection of perceptual mismatch or attentional processes in the visual modality (ibid), i.e., some processes possibly involved in perceptual decisions and the triggering of late responses but definitely subsequent to the inhibition of automatic responses. The P3 could for its part index attentional processes involved in the evaluation of a given stimulus in working memory with respect to expectations and task demands, and the updating of stimulus representations (i.e., for adapting cognitive control for the next trial). (see also for instance Gonzalez-Rosa et al., 2013; Huster et al., 2011; Kropotov et al., 2011).

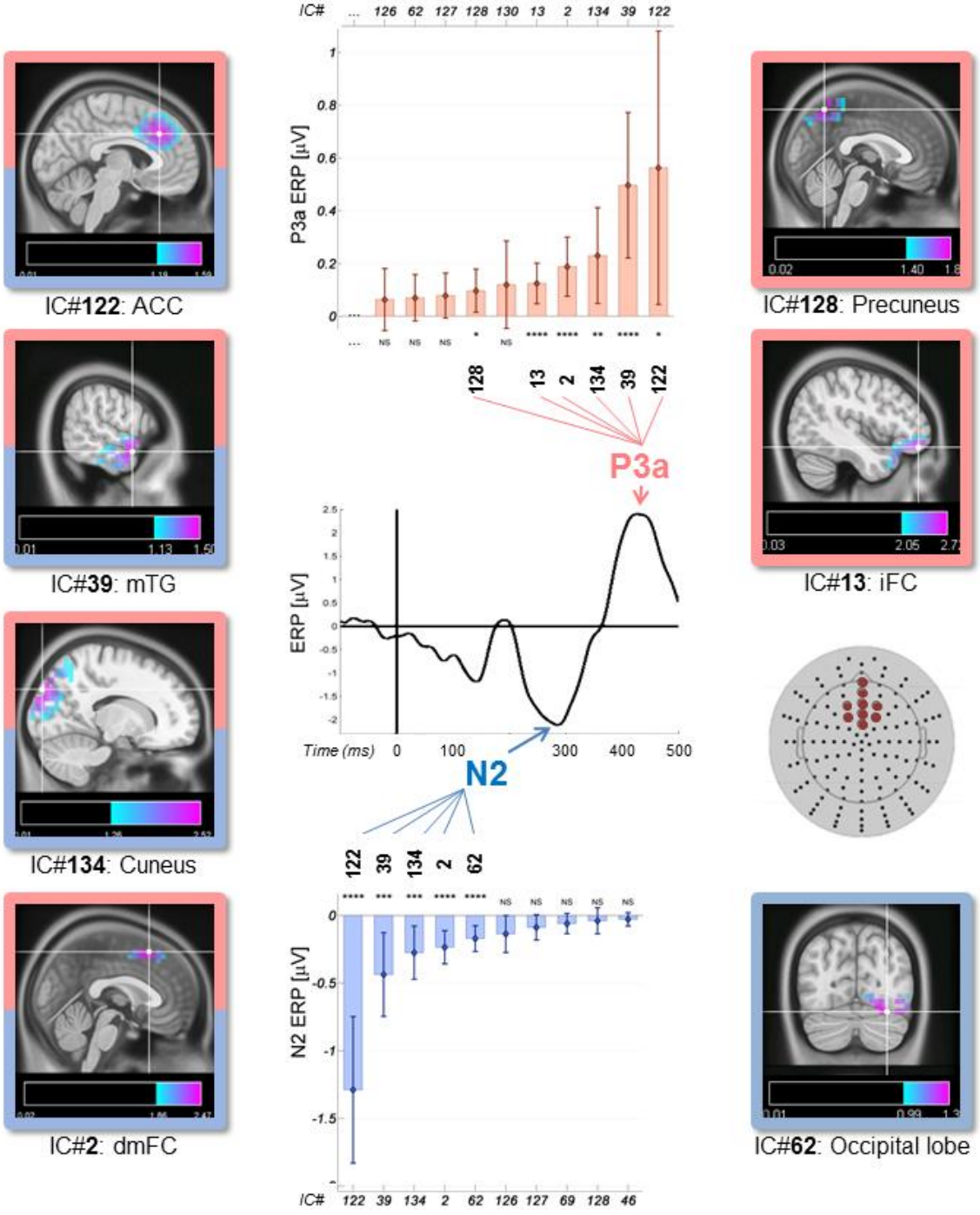

2. Supplementary analyses

a. Objective

Inherent in group BSS analyses, the linear regressions presented in the main text compare the average effect with respect to the inter-trial variability. This may include a bias because the ERPs for each class of RT have been calculated without the assurance that each subject contributes equally to each class. To control for this possible bias, we performed complementary correlational analyses *i)* at the individual level by using linear regressions comparing each single-subject average effect with respect to its inter-trial variability, and *ii)* at the group level by using linear regressions comparing the group average effect with respect to its inter-individual variability. These analyses were applied to the dMF170 ERP/RT correlation in order to assess more thoroughly the relation between the main behavioral and electrophysiological markers of response initiation control. They were also applied to the meaningful spectral data (ERP/delta-thêta power and ERP/alpha power) in order to assess more thoroughly the positive relation between delta-thêta activity and the amplitude of the dMF170, and the negative relation between alpha activity and the amplitude of the dMF170. For these spectral analyses, we considered separately the time-locked and the phase-locked activities of the dMF170 to ensure that, at the individual level, the burst of alpha power is not just the spectral representation of the ERP but that the ERP is rather accounted for by delta/theta activity as suggested by the group BSS analyses.

However, switching from group BSS analyses to single-subject analyses requires substantial amendments of data processing methods.

b. Methods

Spatial filtering of the dMF170 component.

Group BSS (gBSS) spatial filters are obviously optimized for group level analyses, not for single subject analyses which are more sensitive to outlier trials. Indeed, gBSS spatial filters extract the source signal of interest at the identified location while filtering interfering sources estimated at the group level. To switch from gBSS spatial filter to single subject filter, an appropriate strategy consists in creating a spatial filter that extracts the signal from the same location, but can estimate interfering sources at the trial level. This can be done by using Linearly Constrained Minimum Variance (LCMV, Van Veen et al, 1997) and Synthetic Aperture Magnetometry (SAM, Robinson and Vrba, 1998) beamformer techniques in combination with the spatial information estimated at the group level in the gBSS mixing matrix (Fig. S3):

Given the classical linear mixing model in BSS:

$$x = A.s \qquad \text{(equ. 1)}$$

where $x = [x_1 x_2 \dots x_m]$ m-channel scalp EEG signals are generated by the linear mixing of m independent sources $s = [s_1 s_2 \dots s_m]$ and A is the mixing matrix.

gBSS estimates one unmixing matrix W and m-sources such as:

$$\hat{s} = W.x \qquad \text{(equ. 2)}$$

and (where the upper script + denotes the Moore-Penrose pseudo inverse):

$$\hat{A} = W^{+} \qquad \text{(equ. 3)}$$

Each row of $W$is a spatial filter for estimating a source / an independent component and each column of the estimated mixing matrix $\hat{A}$ can be considered as a spatial projection of a source.

Considering one component i, with the mixing vector $\hat{A}_i$ and the group spatial filter W_i, the gBSS spatial filter W_i is optimized for group level analyses, but is not optimal for individual analyses especially because interfering sources are estimated blindly at the group level. For individual analyses, we estimated the interfering sources at the trial level by means of LCMV/SAM beamformer techniques to recompute the spatial filter W_i at each trial j:

$$W_i(j) = Cr_j^{-1} A_i \left[A_i^T Cr_j^{-1} A_i \right]^{-1} \qquad \text{(equ. 4)}$$

where Cr_j is the regularized data covariance matrix, computed for the trial j :

$$Cr_j = C_j + \mu . diag(C_j) \qquad \text{(equ. 5)}$$

where C_j is the data covariance matrix computed for the trial j, μ the Backus-Gilbert regularization parameter (=10) and $diag(C_j)$ the matrix of the diagonal elements of C_j (the diagonal matrix of sensor noise).

Figure S3: dMF170 ERPs back-transformed to the electrode space and averaged on channel C23/Fcz after optimization of spatial filtering for individual analyses

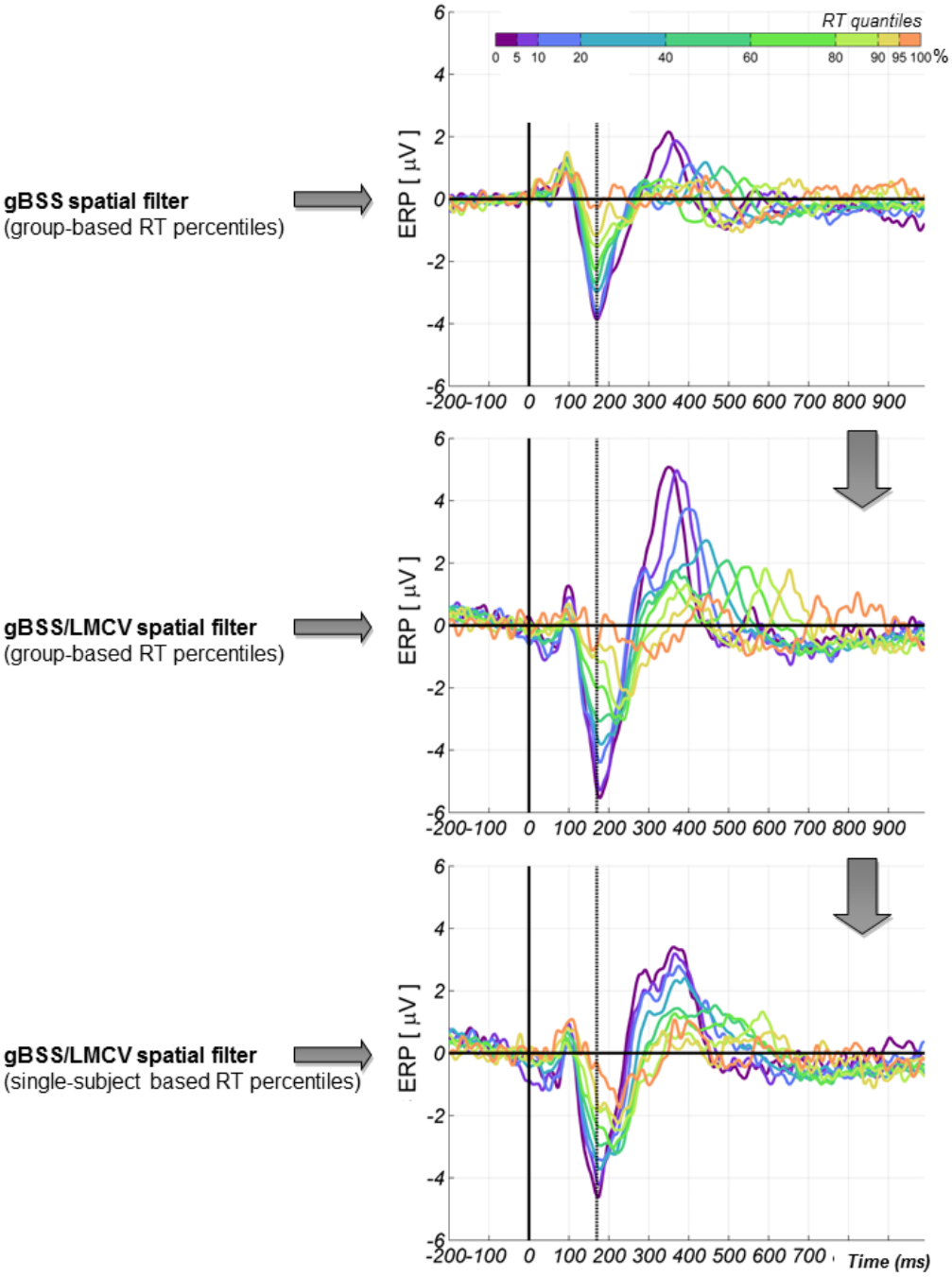

The resulting spatial filter extracts the signal at the same cortical location, oriented in the same direction as the gBSS spatial filter. Yet, interferences are filtered at the trial level, leading to more accurate results for the single subject analyses. These spatially filtered data were back projected to the electrode space, and displayed on the electrode that mostly contributes to the source variance (C23/Fcz, Fig. S3).

Single trial estimation of the dMF170 time-locked and phase-locked delta-theta and alpha power

Spatially filtered data were band pass filtered in the delta/theta (1.5-7.5 Hz) and alpha (7.5-13.5 Hz) bands using the zero-phase Elliptic Infinite Impulse Response (IIR) filters designed for the main gBSS study.

In order to estimate the time-locked spectral power, 170 ms after stimulus onset, the complex analytic signal of each filtered trial was derived by the Hilbert transform (Matlab™ hilbert function) and the instantaneous amplitude envelope was computed by taking the absolute magnitude of the complex waveform. Then, estimated power values at t=170ms were averaged.

In order to estimate the phase-locked spectral power, band-pass filtered data were first averaged across trials, removing all out-of-phase activities. Then, the complex analytic signals of the averaged signals were derived by the Hilbert transform and the instantaneous amplitude envelopes were computed by taking the absolute magnitude of the complex waveforms. The resulting signals represent the amount of power in the filtered frequency band that contributes to the ERP.

Single-subject correlation analyses

The relation between RT and the amplitude of the different signals extracted from the dMF170 (ERP, Time-Locked and Phase-Locked spectral activities) were assessed by means of Pearson correlations. These calculations have been applied after Vincentization of RT data based, for each subject, on its own RT distribution. Trials with an appropriate motor response were partitioned into 9 classes (RT < 5th < 10th < 20th < 40th < 60th < 80th < 90th < 95th < 100th percentile of the subject RT distribution) and averaged. The linear relationship between RT and the cortical activity under scrutiny was tested with a one-tailed Pearson correlation test, the a priori sign of the correlation being determined by the results of the original gBSS study.

Group analyses

Linear regressions comparing the group average effect with respect to its inter-individual variability were performed. Single subject data were Z-transformed to ensure equal contribution of all subjects. Then, data were averaged for each class of RT. Finally, the linear relationship between the subject relative Z-transformed activity and the RT-classes was tested by means of a one-tailed Pearson correlation test, the a priori sign of the correlation being determined by the results of the original group BSS study.

c. Results

dMF170 ERP/RT correlations

Results are displayed in Fig. S4.

Group analysis: Pearson correlation=0.97, p< .001

Single-subject analyses: Coherent Pearson correlation for 17/20 subjects, significant for 13 subjects

Figure S4: Individual correlations of dMF170 ERP amplitude and RT. Individual linear regressions are presented in grey in the lower part of the graph. The group linear regression based on inter-individual variability is represented in black. Individual r and p values are presented in the upper part.

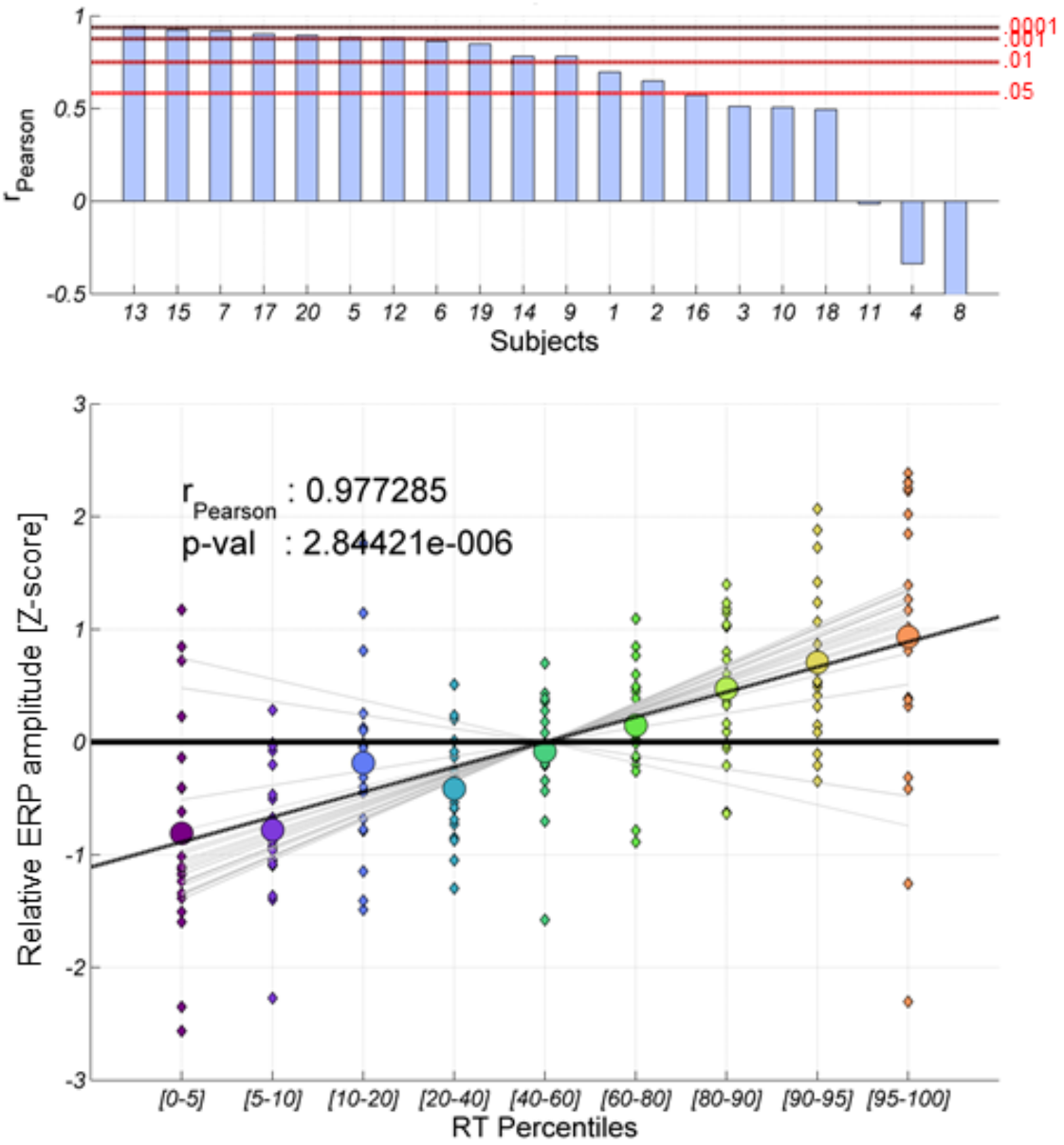

dMF170 time-locked spectral activity/RT correlations

Delta/Thêta

Group analysis: not significant

Single-subject analyses: Significant for 2/20 subjects

Alpha

Group analysis: Pearson correlation=0.88, p< .001

Single-subject analyses: Coherent Pearson correlation for 14/20 subjects, significant for 6 subjects

Figure S5: Individual correlations of time-locked spectral power and RT. Individual linear regressions are presented in grey in the lower part of the graph. The group linear regression based on inter-individual variability is represented in black. Individual r and p values are presented in the upper part.

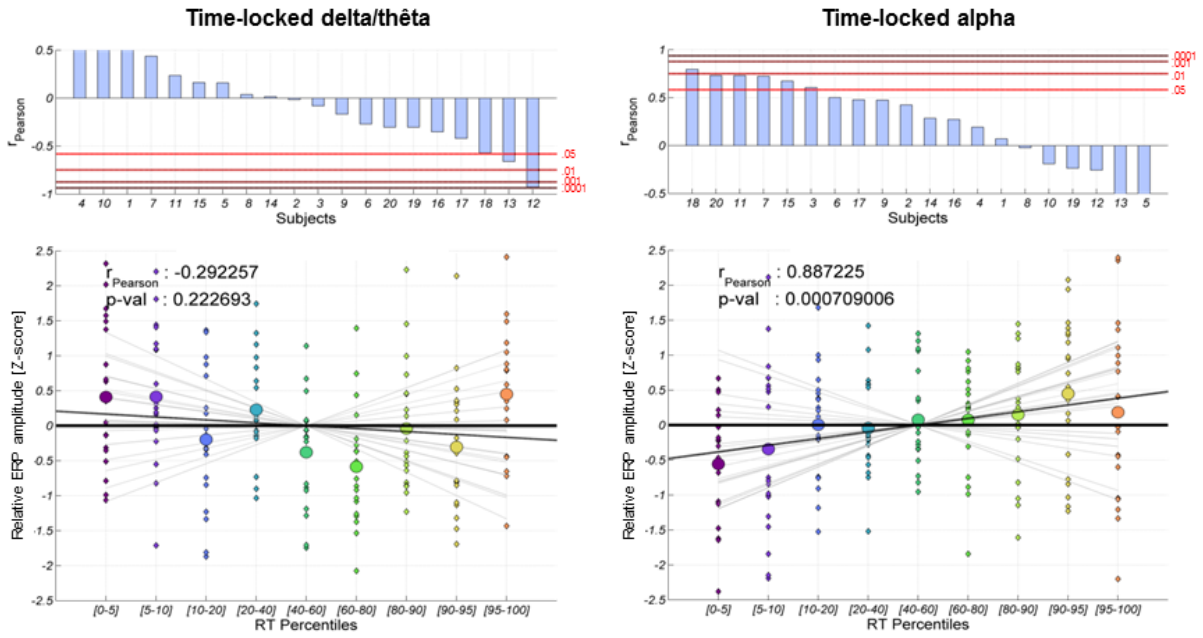

dMF170 phase-locked spectral activity/RT correlations

Delta/Thêta

Group analysis: Pearson correlation=-0.9, p< .001

Single-subject analyses: Coherent Pearson correlation for 17/20 subjects, significant for 8 subjects

Alpha

Group analysis: not significant

Single-subject analyses: Significant for 1/20 subjects

Figure S6: Individual correlations of phase-locked spectral power and RT. Individual linear regressions are presented in grey in the lower part of the graph. The group linear regression based on inter-individual variability is represented in black. Individual r and p values are presented in the upper part.

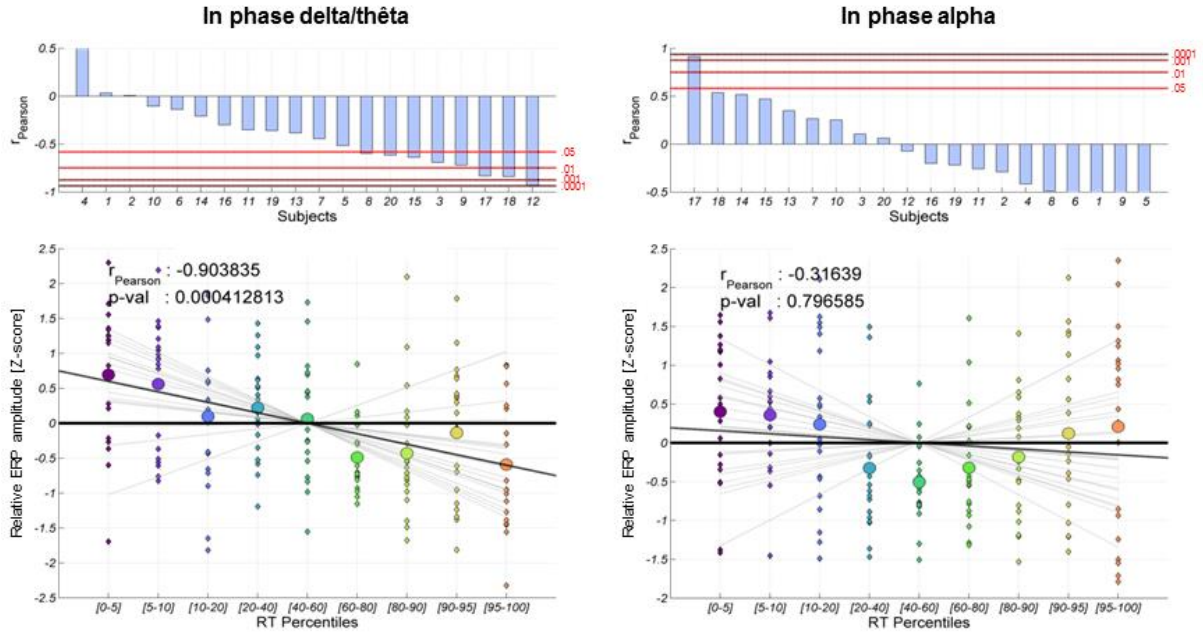

d. Conclusion

The group linear regression based on the inter-individual variability shows that the dMF170 ERP amplitude predicts RT as well as the main gBSS analysis provided in the main text. At the Individual level, a coherent pattern is observed for 17/20 subjects.

Similar group analyses of the spectral properties of the dMF170 confirm that time-locked, not phase-locked, alpha power predicts RT, with coherent individual patterns observed for 14/20 subjects. Conversely, phase -locked, not time -locked, delta/thêta power correlates with RT (negative correlation, with a coherent pattern observed for 17/20 subjects).

The dMF170 ERP is accounted for by delta/theta activity. Its amplitude predicts RT. The attenuation of the ERP is unequivocally attributable to the burst in alpha power.

3. Supplementary references

Gonzalez-Rosa JJ, Inuggi A, Blasi V, Cursi M, Annovazzi P, Comi G, Falini A, Leocani L (2013): Response competition and response inhibition during different choice-discrimination tasks: evidence from ERP measured inside MRI scanner. Int J Psychophysiol 89:37–47.

Huster RJ, Eichele T, Enriquez-Geppert S, Wollbrink A, Kugel H, Konrad C, Pantev C (2011): Multimodal imaging of functional networks and event-related potentials in performance monitoring. NeuroImage 56:1588–1597.

Huster RJ, Enriquez-Geppert S, Lavallee CF, Falkenstein M, Herrmann CS (2013): Electroencephalography of response inhibition tasks: functional networks and cognitive contributions. Int J Psychophysiol 87:217–233.

Kropotov JD, Ponomarev VA, Hollup S, Mueller A (2011): Dissociating action inhibition, conflict monitoring and sensory mismatch into independent components of event related potentials in GO/NOGO task. NeuroImage 57:565–575.

Robinson SE, Vrba J (1999): Functional neuroimaging by synthetic aperture magnetometry (SAM), In Recent Advances in Biomagnetism, Yoshimoto T, Kotani M, KurikiS, Karibe H, Nakasato N (editors), p302-305, Sendai, Japan, 1999.

Van Veen BD, Van Drongelen W, Yuchtman M, Suzuki A (1997): Localization of brain electrical activity via linearly constrained minimum variance spatial filtering. IEEE Trans Biomed Eng 44:867–880.

Zhang Y, Tang AC, Zhou X (2014): Synchronized network activity as the origin of a P300 component in a facial attractiveness judgment task. Psychophysiology 51:285–289.